ACCELERON AEROSPACE JOURNAL (AAJ)
E-ISSN: 2583-9942 (Online) | Accessible at www.acceleron.org.in
Volume 6, Issue 2, (pp.1714-1722)
Article ID: AAJ.11.2106-2608
White Paper
https://doi.org/10.61359/11.2106-2608

Electro Magnetic Curvature Theory – Working Summary

Wayne Griffiths *

Principal Researcher, Deep-Space Habitat and Propulsion Systems, AEMS LLC.

Abstract: We present a governed, falsifiable experimental framework for probing whether quantum-coherent electromagnetic systems can generate measurable spacetime curvature. The proposed apparatus consists of a counter-rotating toroidal stack of high-temperature superconducting rings (YBCO/BSCCO, 10–15 cm diameter, 500–1000 A, 1–5 T), an axial superconducting electromagnetic lens for directional field bias, and a cryogenic high-vacuum environment operating below 10^{-6} torr. This configuration is designed to produce an anisotropic stress–energy distribution topologically analogous to the boundary structure of warp-metric solutions in the weak-field, linearized regime, without invoking exotic matter or modifications to established physics. The detection framework employs dual-channel readout, a high-precision interferometer (phase sensitivity ~10^{-15} rad) and a torsion balance (torque resolution ~10^{-12} N·m), to search for gravitomagnetic and frame-dragging-like signatures with effective angular velocity sensitivity in the range 10^{-16} to 10^{-18} rad/s. The experiment is structured so that both positive detections and null results yield publishable outcomes: either revealing previously unmeasured electromagnetic–gravity coupling in quantum-coherent systems, or establishing the strongest laboratory bounds to date on such interactions. The complete apparatus is estimated at USD 300,000–500,000, with a construction and commissioning timeline of 12–18 months.

Table of Contents

1. Introduction

General relativity relates spacetime curvature to the distribution of energy and momentum through Einstein's field equations. In compact form, these can be written as:

$$G\mu\nu \;=\; (8\pi G \,/\, c^4)\, T\mu\nu$$

where Gμν is the Einstein tensor describing curvature, Tμν is the stress–energy tensor, G is Newton's gravitational constant, and c is the speed of light. In principle, any form of energy–momentum, including electromagnetic fields, contributes to Tμν and therefore to curvature.

For classical electromagnetic fields in vacuum, the energy density is given by:

$$u \;=\; (\varepsilon_0 E^2 \;+\; B^2 \,/\, \mu_0) \,/\, 2$$

where E is the electric field, B is the magnetic field, ε_0 is the vacuum permittivity, and μ_0 is the vacuum permeability. The corresponding stress–energy tensor for the electromagnetic field, Tμν(EM), is well known and can be written in terms of the field tensor Fμν. In practice, however, the curvature generated by laboratory-scale electromagnetic fields is expected to be extremely small. The motivation for this work is not to claim that electromagnetic fields can trivially generate large curvature, but to recognize that modern superconductors, quantum-coherent materials, and precision metrology now allow us to probe regimes that were simply inaccessible when the canonical theory was formulated. The question is not "can we build a warp drive," but rather: can we design a disciplined, falsifiable experiment that measures or bounds electromagnetic contributions to curvature in a quantum-coherent, strongly

*Principal Researcher, Deep-Space Habitat and Propulsion Systems, AEMS LLC. **Corresponding Author:** waynegriffiths9@gmail.com.
Article History: Received: 07-Feb-2026 || Revised: 23-March-2026 || Accepted: 25-March-2026 || Published Online: 30-March-2026.

Copyright © AASPL. Published by Acceleron Aerospace Journal (AAJ), (E-ISSN:2583-9942) with permission. This work is licensed under a Creative Commons Attribution 4.0 International License (CC BY 4.0). For more info, visit www.acceleron.org.in.

ordered system? This document proposes such an experiment. It combines a toroidal superconducting ring stack, an axial electromagnetic lens, a cryogenic and vacuum environment, and a high-precision detection framework to probe possible curvature-like signatures, including gravitomagnetic effects, frame-dragging analogues, and subtle metric perturbations. The architecture is deliberately conservative: it uses only established physics as its starting point, acknowledges all critical unknowns, and is structured so that null results are scientifically valuable.

2. Architectural Skeleton

The proposed apparatus is built around a compact, vertically stacked architecture designed to concentrate electromagnetic energy and momentum in a controlled, anisotropic configuration. The core elements are: a) a toroidal electromagnetic ring stack acting as a "bubble shaper"; b) an axial electromagnetic lens providing directional bias; c) a cryogenic cold stage and vacuum environment; d) a dual-channel detection framework (interferometric and torsion-balance based). The goal of the architectural skeleton is to create a stress–energy distribution that is both experimentally accessible and topologically reminiscent of the boundary structures explored in warp-metric literature, while remaining firmly within the domain of real, testable physics.

2.1 Toroidal EM Ring Stack — Bubble Shaper

At the heart of the apparatus is a pair of high-temperature superconducting rings arranged in a toroidal stack. Each ring has a diameter in the range of 10–15 cm and a thickness of approximately 1.5–2 cm. The rings are mounted horizontally, one above the other, with a vertical separation of 6–8 cm. They are cooled to superconducting temperatures (around 77 K for YBCO-class materials) and driven with currents in the 500–1000 ampere range, producing magnetic fields on the order of 1–5 tesla. The rings are mounted on independent rotation stages, allowing them to counter-rotate at angular velocities corresponding to 10–100 revolutions per second. This counter-rotation is not intended to generate classical centrifugal forces of interest, but to create an anisotropic, time-varying stress–energy distribution and to suppress net mechanical torque transfer to the environment. The toroidal geometry is chosen to confine the magnetic field and to approximate a "bubble-like" region of modified stress–energy density.

2.2 Axial EM Lens — Directional Bias

Above the ring stack, aligned with the central vertical axis, is an axial electromagnetic lens. This is implemented as a flat superconducting disk approximately 8 cm in diameter and 1 cm thick, capable of supporting static or pulsed magnetic fields in the 0.5–2 tesla range. The lens is supported by thin, non-conductive struts attached to the chamber wall and is electrically driven through a dedicated feedthrough. The role of the axial lens is to introduce a directional bias in the electromagnetic field configuration, creating a region of relative compression ahead of the apparatus and relative relaxation behind it, in analogy with the boundary topology of certain warp-metric solutions. No claim is made that this reproduces a full warp metric; rather, the lens provides a controlled way to break symmetry and to study how directional field structures couple to the surrounding spacetime in the weak-field, linearized regime.

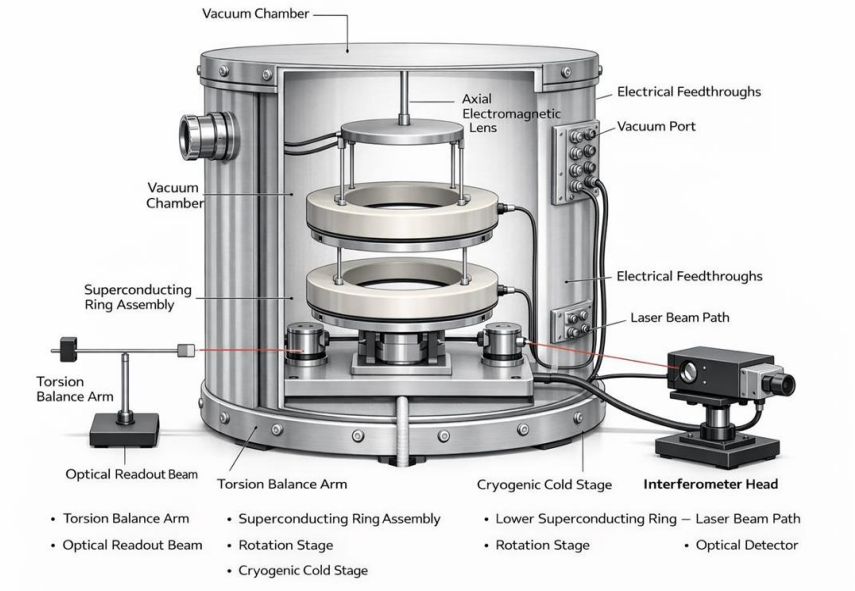

Acceleron Aerospace Journal || AAJ.11.2106-2608
Volume 6, Issue 2, pp (1714-1722)
E-ISSN- 2583-9942
https://dx.doi.org/10.61359/11.2106-2608

Check for updates

3. Why this architecture holds together

The architecture is designed to be simultaneously: topologically informed by warp-metric boundary structures – grounded in standard general relativity and electromagnetism – compatible with existing experimental precedents – falsifiable with current or near-term laboratory capabilities.

3.1 Topological Match to Alcubierre Boundary

The Alcubierre warp metric and its successors describe spacetime configurations in which a "bubble" of nearly flat spacetime is embedded in a region of highly curved spacetime, with compression in front and expansion behind. While these solutions require exotic matter in their original formulations, they provide a useful topological template. The toroidal ring stack and axial lens are arranged to approximate a simplified version of this boundary structure. The rings generate a concentrated, toroidal electromagnetic energy density, while the axial lens introduces a directional gradient. In the weak-field, linearized regime, the metric perturbations hμν can be related to the stress–energy tensor via the linearized Einstein equations:

$$h\mu\nu \;=\; -(16\pi G \,/\, c^4)\,(T\mu\nu \;-\; ½\,\eta\mu\nu\, T)$$

where □ is the d'Alembert operator, ημν is the Minkowski metric, and T is the trace of the stress–energy tensor. The architecture is chosen so that Tμν has a non-trivial spatial structure that can, in principle, generate small but structured metric perturbations.

3.2 Uses Only Real Physics

No exotic matter, negative energy densities, or speculative modifications of general relativity are assumed. The starting point is: standard Einstein field equations – standard electromagnetic stress–energy tensor – standard gravitoelectromagnetism (GEM) in the weak-field limit – standard superconductivity and London theory.

In the GEM approximation, the metric is linearized around flat spacetime, and the gravitational field is described in terms of gravitoelectric and gravitomagnetic fields, analogous to electric and magnetic fields in electromagnetism. The gravitomagnetic field Bg is sourced by mass currents and, in certain formulations, by energy–momentum flows. The frame-dragging angular velocity Ωg near a rotating mass distribution can be estimated as:

$$\Omega g \sim GJ \,/\, (c^2\, r^3)$$

where J is the angular momentum and r is the characteristic distance. In this experiment, the effective J includes contributions from the circulating superconducting currents and the rotating mass of the rings. The expected Ωg is extremely small, but with sufficient integration time and careful null controls, it may be possible to bound or detect such effects.

3.2 Canon Integration

The architecture is explicitly designed to sit within, and be evaluated against, the existing canon of: warp-metric theory (Alcubierre, Bobrick & Martire, and others); gravitoelectromagnetism and frame-dragging experiments; superconducting gravito-magnetic experiments (including controversial ones).

3.2.1 Precision interferometry and torsion-balance measurements

Section 2B summarizes the most relevant experimental and theoretical precedents and shows how this apparatus is positioned to either extend or constrain them.

3B. Experimental Precedent & Theoretical Support

Several lines of prior work motivate and constrain this experiment:

Alcubierre (1994) introduced the original warp drive metric, demonstrating that general relativity permits solutions with localized "bubbles" of modified spacetime, albeit requiring exotic matter. – Bobrick and Martire (2021) reformulated warp drives in a more physically grounded way, emphasizing the role of realistic stress–energy distributions and clarifying the limitations and possibilities of "physical warp drives." Tajmar and collaborators (2006 and subsequent work) reported measurements related to the gravitomagnetic London moment in rotating superconductors, suggesting possible couplings between superconductivity and gravito-magnetic fields, though these results remain controversial and have not been universally replicated. Tate et al. (1989) measured the effective mass of Cooper pairs in superconducting rings, providing a precise experimental handle on superconducting charge carriers and their coupling to electromagnetic fields. – Forward (early 1960s) and others

explored the theoretical and experimental foundations of gravitoelectromagneticism, including the possibility of generating and detecting extremely small gravitomagnetic fields in laboratory settings. This experiment does not assume that any controversial result is correct. Instead, it is designed to: Reproduce or refute gravitomagnetic-like signatures in a new geometry; explore quantum-coherent EM configurations not previously tested; provide clean null results if no effect is present.

4. Critical Unknowns

A credible experiment must foreground its unknowns rather than bury them. The critical unknowns in this architecture are:

Amplification mechanisms

It is unknown whether quantum coherence, macroscopic phase ordering, or topological field configurations can amplify the effective coupling between electromagnetic stress–energy and curvature beyond the naive classical expectation. The experiment is explicitly designed to test for such amplification, but no amplification is assumed.

Coherence length and volume

The effective coherence length and volume over which superconducting and solid-state plasma effects might contribute coherently to any curvature-like signature are not known. The ring dimensions and separation are chosen to maximize the coherent volume within practical constraints, but the true effective volume is an experimental question.

Detection thresholds

The minimum detectable frame-dragging-like signal, phase shift, or torsion-balance deflection depends on the noise floor, integration time, and environmental stability. While the detection framework is designed to reach sensitivities in the range of 10^{-16} to 10^{-18} radians per second for effective frame-dragging rates, the actual thresholds will be established empirically.

Noise sources and systematics

Vibration, thermal drift, electromagnetic interference, and mechanical coupling between rotating components and the environment can all mimic or obscure small signals. The experiment includes null controls and isolation strategies, but the full noise budget itself is a critical unknown to be characterized.

Scaling behavior

Even if a small effect is observed, it is unknown how it scales with current, field strength, ring size, rotation rate, or material properties. The Phase 1 apparatus is designed to establish whether any effect exists at all and to provide initial scaling data, but full scaling laws would require follow-on experiments.

The experiment is therefore framed not as a guaranteed detection, but as a disciplined attempt to map these unknowns into quantitative constraints.

5. Forward Roadmap

The forward roadmap is structured into four phases:

Phase 1: Design and simulation (3–6 months) Phase 2: Construction and commissioning (12–18 months) Phase 3: Initial testing and null characterization (6–12 months) Phase 4: Full experimental campaign and publication (12–18 months). This yields a total project duration of approximately 33–54 months (3–4.5 years), depending on resource availability and iteration cycles.

5.1 Full Stress–Energy Tensor Derivation

A complete derivation of the stress–energy tensor for the apparatus requires modeling the electromagnetic fields generated by the superconducting rings and axial lens – computing the corresponding Tμν(EM) in the laboratory frame – incorporating contributions from mass currents and mechanical rotation – applying the linearized Einstein equations to estimate metric perturbations hμν

The electromagnetic stress–energy tensor can be written in terms of the field tensor Fμν as:

$$T\mu\nu(EM) = (1 / \mu_0)\,(F\mu\alpha\, F\nu\,\alpha - \tfrac{1}{4}\,\eta\mu\nu\, F\alpha\beta\, F\alpha\beta)$$

Acceleron Aerospace Journal || AAJ.11.2106-2608
Volume 6, Issue 2, pp (1714-1722)
E-ISSN- 2583-9942
https://dx.doi.org/10.61359/11.2106-2608

Check for updates

In the weak-field limit, the resulting metric perturbations are expected to be extremely small, but this derivation provides the baseline against which any observed effect must be compared. The goal is not to claim large curvature, but to quantify the classical expectation and to identify any deviations..

5.2 Amplification Mechanisms

Several speculative but testable amplification mechanisms motivate the choice of superconducting and solid-state plasma materials: macroscopic quantum coherence and phase rigidity – topological field configurations in toroidal geometries – Berry curvature effects in solid-state systems – possible enhancement of gravitomagnetic-like responses in superconductors. These mechanisms are not assumed; they are hypotheses to be constrained. The experiment is designed so that: if no amplification exists, the result is a strong null bound – if any amplification exists, even at very small levels, it may be detectable with sufficient integration time.

5.3 Phase 1 Apparatus Specifications

The proposed experiment can be constructed entirely from commercially available components and standard laboratory infrastructure. The apparatus consists of four major subsystems: the superconducting ring assembly, the axial electromagnetic lens, the vacuum and cryogenic environment, and the detection suite.

Together, these form a compact, high-signal platform for probing electromagnetic contributions to spacetime curvature. The superconducting ring assembly is built from high-temperature superconductors such as YBCO or BSCCO. The rings have diameters in the 10–15 cm range and operate at currents between 500 and 1000 amperes, producing magnetic fields of approximately 1–5 tesla. The rings are counter-rotated at 10–100 Hz to generate the required anisotropic stress–energy distribution and to suppress mechanical torque transfer. The mechanical torque associated with the rotating rings is on the order of 10^{-3} to 10^{-2} newton-metres, depending on mass and rotation rate, and is managed through symmetric mounting and isolation.

The axial electromagnetic lens consists of an 8 cm superconducting disk capable of producing static or pulsed fields in the 0.5–2 tesla range. Its purpose is to introduce a directional bias in the electromagnetic field structure, creating forward compression and rear relaxation analogous to the boundary topology of a warp-like metric in the weak-field limit. The vacuum and cryogenic environment is provided by a chamber approximately 50 cm in diameter and 60 cm in height, operating at pressures below 10^{-6} torr. The system includes both active and passive vibration isolation to ensure interferometric stability. Cooling is achieved using liquid nitrogen or a closed-cycle cryocooler, maintaining the superconducting components at approximately 77 K.

The detection suite includes a high-precision interferometer with phase sensitivity on the order of 10^{-15} radians, a torsion balance capable of resolving torques down to approximately 10^{-12} newton-metres, and gyroscopes or equivalent angular sensors with effective drift rates below 10^{-16} radians per second. A second-phase upgrade may incorporate atomic clocks with fractional timing stability of 10^{-16} for time-dilation-like measurements. For a representative configuration, the expected frame-dragging-like effective angular velocity from classical GEM estimates is in the range of 10^{-16} to 10^{-18} radians per second, implying integration times from hours to weeks depending on the noise floor.

The complete apparatus, including materials, cryogenics, vacuum systems, detection instrumentation, and labour, is estimated to cost between 300,000 and 500,000 USD. Construction and commissioning are expected to require 12–18 months, with initial data collection beginning shortly thereafter. The Dual-Ring Habitat includes two dedicated experimental bays capable of hosting this apparatus in long-duration microgravity, with independent cryogenic, vacuum, and vibration-isolation systems to prevent interference with the habitat's superconducting levitation coils.

6. Gravito Electromagnetism in Superconductors

Gravitoelectromagnetism (GEM) provides a useful linearized framework for describing weak gravitational fields in a form analogous to Maxwell's equations. In this picture, mass and energy currents generate a gravitomagnetic field Bg, and moving test masses experience gravitomagnetic forces analogous to magnetic Lorentz forces.

In superconductors, the London equations describe how supercurrents respond to electromagnetic fields. There have been theoretical proposals and experimental claims suggesting that superconductors might exhibit enhanced coupling to gravitomagnetic fields, including the so-called gravitomagnetic London moment. While these claims remain controversial, they motivate a careful, falsifiable experiment.

Gravitomagnetic London Moment

The classical London moment describes the magnetic field generated by a rotating superconductor. In simplified form, the magnetic field B generated by a rotating superconducting body with angular velocity Ω can be written as:

$$B \approx -(2m / q)\, \Omega$$

where m is the Cooper pair mass and q is the Cooper pair charge. Some theoretical extensions and experimental claims have suggested an analogous gravitomagnetic London moment, in which a rotating superconductor might generate a gravitomagnetic field proportional to its angular velocity.

In a GEM-like formulation, a gravitomagnetic field Bg associated with a rotating mass–energy distribution can be written schematically as:

$$Bg \sim (G / c^2)\, (J / r^3)$$

where J is the angular momentum and r is the characteristic distance. The experiment described here does not assume any enhancement beyond this classical expectation, but it is designed to be sensitive to any anomalous gravitomagnetic-like signals that might arise in a superconducting configuration.

Gravitomagnetic Meissner Like Response

The Meissner effect describes the expulsion of magnetic fields from the interior of a superconductor. Some speculative models have proposed a gravitomagnetic analogue, in which superconductors might partially expel or modify external gravitomagnetic fields. While there is no consensus that such an effect exists, the combination of rotating superconducting rings and precision detection instruments provides an opportunity to search for any Meissner-like response in the gravitomagnetic sector.

The experiment is structured so that:

if no gravitomagnetic London or Meissner-like effects exist, the result is a strong null bound – if any such effects exist at small levels, they may manifest as tiny but structured signals in the interferometric or torsion-balance channels

7. Solid State Plasma and Berry Curvature

The detection framework is built around two primary channels:

an interferometric channel sensitive to tiny path-length or phase changes – a torsion-balance channel sensitive to tiny forces or torques The goal is to detect, or place bounds on, any curvature-like or gravitomagnetic-like signatures associated with the operation of the apparatus.

8. Detection Framework

The detection framework is built around two primary channels: an interferometric channel sensitive to tiny path-length or phase changes – a torsion-balance channel sensitive to tiny forces or torques. The goal is to detect, or place bounds on, any curvature-like or gravitomagnetic-like signatures associated with the operation of the apparatus.

Quantum Specific Null Controls

Null controls are essential to distinguish genuine curvature-like signals from electromagnetic, mechanical, or thermal artefacts. The experiment includes runs with superconducting rings unpowered but rotating; runs with rings powered but not rotating; runs with normal (non-superconducting) conductors in place of superconductors; runs with the axial lens disabled; runs with dummy loads replacing the ring assembly. These controls are designed to isolate purely mechanical effects; purely electromagnetic coupling to the detection instruments; thermal drift and vibration; systematic biases in the interferometer and torsion balance.

Acceleron Aerospace Journal || AAJ.11.2106-2608
Volume 6, Issue 2, pp (1714-1722)
E-ISSN- 2583-9942
https://dx.doi.org/10.61359/11.2106-2608

Check for updates

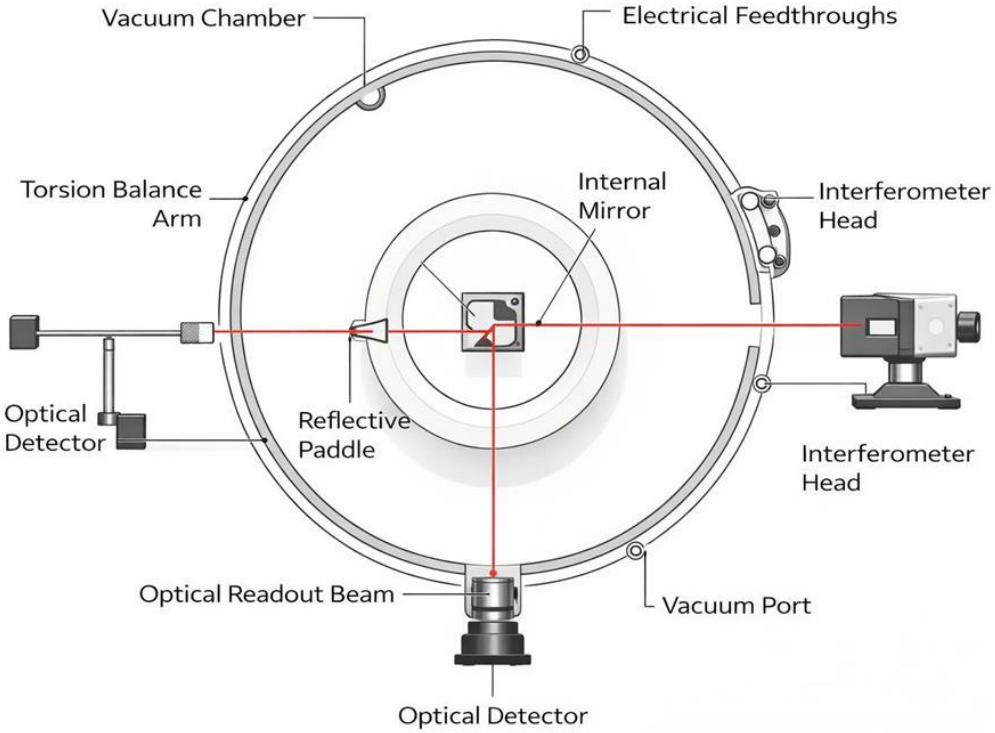

Detection Thresholds & Sensitivity Ladder

The detection ladder is structured in tiers:

Tier 1: Gross anomalies These would include large, easily detectable phase shifts, torque signals, or gyroscopic anomalies. The apparatus is not designed with the expectation of such effects, but it would detect them if present.

Tier 2: Weak but resolvable signals These correspond to effective frame-dragging-like angular velocities in the range of approximately 10^{-14} to 10^{-16} radians per second, or equivalent phase shifts and torque signals. With realistic noise floors and integration hours of time to days, such signals could be resolved if they exist.

Tier 3: Near-limit signals These correspond to effective angular velocities in the range of approximately 10^{-16} to 10^{-18} radians per second. Detection at this level would require long integration times (days to weeks), careful environmental control, and rigorous null analysis.

Tier 4: Null bounds If no signal is detected above the noise floor, the experiment will establish upper bounds on any curvature-like or gravitomagnetic-like effects associated with the apparatus. These bounds will be expressed in terms of effective frame-dragging rates, phase shifts, and torque limits, and will be directly comparable to GEM-based predictions.

9. Risk Mitigation and Publication Pathway

The primary risks are: no detectable effect (null result); ambiguous signals dominated by noise or systematics; difficulty in reproducing results across different laboratories

These risks are mitigated by designing the experiment so that null results are scientifically valuable; implementing multiple, independent detection channels; using conservative, well-understood materials and components; documenting the apparatus and procedures in sufficient detail for replication

The publication pathway includes initial methods and apparatus paper; results paper reporting either detection or null bounds; follow-up papers exploring scaling, materials variations, or upgraded detection schemes.

10. Strategic Timing & Competitive Landscape

The timing of this experiment is shaped by: The maturity of high-temperature superconductors and cryogenic systems; the availability of high-precision interferometry and torsion-balance techniques; renewed interest in warp-metric theory and gravitoelectromagnetism; the emergence of deep-tech accelerators and space-focused research programs. The competitive landscape includes both theoretical and experimental efforts in: precision tests of general relativity laboratory searches for new interactions; advanced propulsion concepts; quantum materials and topological phases. This experiment is positioned not as a competitor to large-scale gravitational wave observatories or cosmological tests, but as a complementary, laboratory-scale probe of a specific, underexplored question.

11. Collaboration Model

The proposed collaboration model distinguishes clearly between:

Contributions from the proposing team:

theoretical framework and architecture – detailed experimental design – stress–energy and GEM modeling data analysis methods and interpretation – documentation and publication drafting

Requirements from the host institution or laboratory: cryogenic infrastructure (liquid nitrogen or cryocoolers); high-vacuum systems capable of reaching below 10^{-6} torr; precision interferometry and torsion-balance equipment or equivalent; mechanical workshop and electronics support; laboratory space with vibration and electromagnetic noise control.

Timeline:

Phase 1: Design and simulation, 3–6 months Phase 2: Construction and commissioning, 12–18 months Phase 3: Initial testing and null characterization, 6–12 months Phase 4: Full experimental campaign and publication, 12–18 months Total project duration: approximately 33–54 months (3–4.5 years), depending on resource allocation and iteration cycles.

12. Why Einstein Never Finished It

Einstein provided the framework that relates curvature to stress–energy, but he did not have access to: superconductors; high-temperature quantum materials; modern interferometry; ultra-high vacuum systems; digital data acquisition and analysis. The parameter space accessible to a 21st-century laboratory is fundamentally different from that of the early 20th century. This experiment does not claim to "complete" Einstein's work, but it does aim to explore a corner of the theory that was, in practice, experimentally inaccessible during his lifetime.

13. Conclusion

This document has outlined a governed, falsifiable, and experimentally grounded architecture for probing electromagnetic contributions to spacetime curvature in a quantum-coherent, superconducting system. The apparatus is compact, buildable with existing technology, and designed so that both positive and null results are scientifically valuable.

The key features are:

A toroidal superconducting ring stack acting as a bubble-shaping stress–energy source; an axial electromagnetic lens providing directional bias; a cryogenic and vacuum environment compatible with high-precision measurements; a dual-channel detection framework with interferometric and torsion-balance readout; a clear roadmap, risk mitigation strategy, and publication pathway. The experiment does not assume exotic physics. It starts from standard general relativity, standard electromagnetism, and standard superconductivity, and asks a disciplined question: can a carefully engineered, quantum-coherent electromagnetic system produce measurable curvature-like signatures, or can we place strong new bounds on such effects? Either outcome advances the field.

Acceleron Aerospace Journal || AAJ.11.2106-2608
Volume 6, Issue 2, pp (1714-1722)
E-ISSN- 2583-9942
https://dx.doi.org/10.61359/11.2106-2608

14. References

[1] Alcubierre, M. (1994). The warp drive: Hyper-fast travel within general relativity. Classical and Quantum Gravity, 11(5), L73–L77. https://doi.org/10.1088/0264-9381/11/5/001.

[2] Bobrick, A., & Martire, G. (2021). Introducing physical warp drives. Classical and Quantum Gravity, 38(10), 105009. https://doi.org/10.1088/1361-6382/abdf6e.

[3] Tajmar, M., Plesescu, F., Marhold, K., & de Matos, C. J. (2006). Experimental detection of the gravitomagnetic London moment. arXiv. https://arxiv.org/abs/gr-qc/0603033.

[4] Tate, J., Cabrera, B., Felch, S. B., & Anderson, J. T. (1989). Precise determination of the Cooper-pair mass. Physical Review Letters, 62(8), 845–848. https://doi.org/10.1103/physrevlett.62.845.

[5] Forward, R. L. (1961). General relativity for the experimentalist. Proceedings of the IRE, 49(5), 892–904. https://doi.org/10.1109/JRPROC.1961.287932.

[6] Podkletnov, E., & Nieminen, R. (1992). A possibility of gravitational force shielding by bulk $YBa_2Cu_3O_{7-x}$ superconductor. Physica C: Superconductivity, 203(3–4), 441–444. https://doi.org/10.1016/0921-4534(92)90055-H.

15. Conflict of Interest

The author declares no competing conflict of interest.

16. Funding

No funding was issued for this research.